

Braidio: An Integrated Active-Passive Radio for Mobile Devices with Asymmetric Energy Budgets

Pan Hu, Pengyu Zhang, Mohammad Rostami, Deepak Ganesan
College of Information and Computer Sciences
University of Massachusetts, Amherst, MA 01003
{panhu, pyzhang, mrostami, dganesan}@cs.umass.edu

Abstract

While many radio technologies are available for mobile devices, none of them are designed to deal with asymmetric available energy. Battery capacities of mobile devices vary by up to three orders of magnitude between laptops and wearables, and our inability to deal with such asymmetry has limited the lifetime of constrained portable devices.

This paper presents a radically new design for low-power radios — one that is capable of dynamically splitting the power burden of communication between the transmitter and receiver in proportion to the available energy on the two devices. We achieve this with a novel carrier offload method that dynamically moves carrier generation across end points. While such a design might raise the specter of a high-power, large form-factor radio, we show that this integration can be achieved with no more than a BLE-style active radio augmented with a few additional components. Our design, Braidio is a low-power, tightly integrated, low-cost radio capable of operating as an active and passive transceiver. When these modes operate in an interleaved (braided) manner, the end result is a power-proportional low-power radio that is able to achieve 1:2546 to 3546:1 power consumption ratios between a transmitter and a receiver, all while operating at low power.

CCS Concepts

•Networks → Network architectures; Wireless access networks;

Keywords

Backscatter; Wireless; Architecture; Asymmetric; Energy

Permission to make digital or hard copies of all or part of this work for personal or classroom use is granted without fee provided that copies are not made or distributed for profit or commercial advantage and that copies bear this notice and the full citation on the first page. Copyrights for components of this work owned by others than ACM must be honored. Abstracting with credit is permitted. To copy otherwise, or republish, to post on servers or to redistribute to lists, requires prior specific permission and/or a fee. Request permissions from permissions@acm.org.

SIGCOMM '16, August 22-26, 2016, Florianopolis, Brazil

© 2016 ACM. ISBN 978-1-4503-4193-6/16/08...\$15.00

DOI: <http://dx.doi.org/10.1145/2934872.2934902>

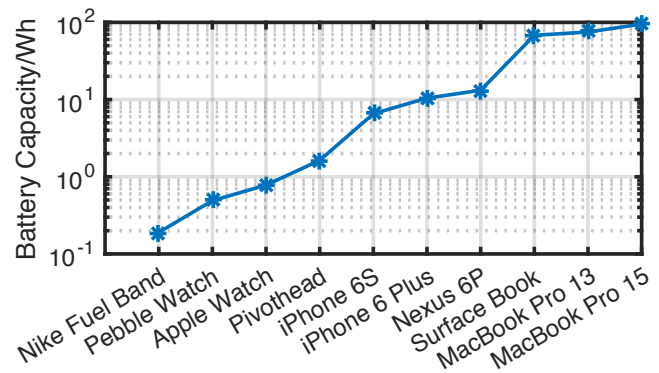


Figure 1: Battery capacity for mobile devices

1. INTRODUCTION

The growing demand for ultra-low power wireless communication has led to a plethora of radio technologies including Bluetooth Low Energy, ZigBee, Z-Wave, and others. While these radios are low-power in nature, we argue that there is one key dimension that existing radio designs have overlooked — asymmetry in energy availability. Battery capacity of mobile devices is roughly proportional of their volume, which in turn varies substantially from laptop-class to smartwatch-class devices. Figure 1 shows the battery capacity for several typical mobile devices [3, 4, 5, 6, 7, 10, 13, 15, 16, 17] (y axis in log scale). A battery on a laptop-class device such as a Macbook Pro or Surface Book is three orders of magnitude larger than a typical fitness band, two orders of magnitude larger than a typical smartwatch, and an order of magnitude larger than a smartphone.

But commercial low-power radios are symmetric in power draw and have minimal ways to accommodate asymmetric energy budgets. Table 1 shows two examples to illustrate — a Bluetooth CC2541 chip [8] supports power ratios (Transmit vs Receive power) of $0.82\times - 1.0\times$ and a Bluetooth Low Energy CC2640 chip [9] supports power ratios between $1.1\times - 1.6\times$. This is a small dynamic range compared to the orders of magnitude gap in energy availability.

In contrast, a radio that is designed to take into account battery asymmetry would be *power-proportional* i.e. the power consumption at the transmitter and receiver would be

Table 1: Transmitter/receiver power ratio of Bluetooth and BLE

	Transmit	Receive	TX/RX Ratio
CC2541	55~60mW	59~67mW	0.82~1.0
CC2640	21~30mW	19mW	1.1~1.6

proportional to the available energy at the end point. A power proportional radio would allow a significant fraction of the energy cost of communication to be offloaded to the device that has more energy i.e. the mobile phone in the above example, thereby increasing the lifetime of the wearable and the overall duration of communication between the devices.

Our design, Braidio (*a braid of radios*), a radically new radio design that is capable of dynamic carrier offload i.e. the ability to dynamically switch the transmission carrier between the transmitter and receiver. The rationale for carrier offload is that the power consumption of communication is dominated by the cost of generating a carrier signal. Active radios generate the carrier at both the transmitter and receiver, therein the near-identical power consumption at both ends. Passive communication systems such as RFIDs generate the carrier solely at the reader end, hence they support highly asymmetric power consumption. Thus, if we were able to combine the architectural building blocks of both active and passive radios, we can design a radio that is capable of moving carrier generation between the two end points. This capability can, in turn, enable power-proportional wireless communication wherein two devices with different battery capacities can multiplex between the different carrier generation modes such that they consume power in proportion to their available energy.

Dynamic carrier offload is compelling, but the reality of designing such a radio is also daunting. Passive backscatter communication is designed to be ultra-low power at the tag, but uses a rather bulky and power-hungry reader that consumes watts of power, not milliwatts. For carrier offload to be practical, we need to be able to move the carrier across end-points while incurring low power consumption.

We tackle this problem through an innovative architecture that integrates the key components of both active and passive radios, in particular carrier generation and self-interference cancelation, while still operating at an end-to-end power consumption comparable to active radios. Our key innovation is the use of passive methods to cancel self-interference, which paves the way for a low-power, yet high-performance, end-to-end design. We are aware of no other attempt at combining active and passive radios into a low-power transceiver that is capable of seamlessly switching between these modes.

Our results show that:

- Braidio can support transmitter–receiver power ratios between 1:2546 to 3546:1 and enables a huge dynamic range of asymmetry to suit a wide range of energy budgets between end points.
- Braidio is low-power and consumes between 16uW – 129mW across the different modes, and is small form-

factor, making it practical for a range of mobile devices from laptops to smartwatches.

- Braidio increases the total bits transmitted by several orders of magnitude when compared with Bluetooth, particularly when there is significant asymmetry in battery levels.

2. ACTIVE AND PASSIVE RADIOS

We start by describing the architectures of active and passive radios, and pinpoint key performance bottlenecks.

2.1 Active Radio Architectures

Active radios like Bluetooth are quite symmetric in nature as shown in Figure 2(a). The transmitter generates the carrier (say 2.4 GHz or 915 MHz), phase shifts the carrier, passes it through a mixer to generate the In-phase (I) and Quadrature (Q) signals, and amplifies the signal via a power amplifier before transmission. At the receiver side, the received signal is amplified with a Low Noise Amplifier, fed into a mixer together with a locally generated carrier, and filtered to recover the I and Q signals.

The reason for the symmetric power consumption is evident when we look at the architectural building blocks. The transmitter and receiver are remarkably similar in terms of the components that they use. Both generate the carrier and have an IQ modulator/demodulator, and these components consume most of the power. Thus, only relatively small differences in power consumption are possible between the transmitter and receiver, primarily through changing the transmit power level.

2.2 Passive Radio Architectures

Passive or Backscatter communication works very differently from active radios. In passive communication, the goal is to ensure that the transmitter (or the tag) is an extremely cheap, low-power and low-complexity device. Thus, backscatter tags avoid power hungry components such as the carrier generator, mixer and low-noise amplifier that we saw in the case of active radios. Instead, the reader takes on much of the complexity, and allows the tag to operate simply by reflecting the carrier signal back to the reader. This system works as follows — the tag tunes and detunes its antenna with its RF transistor, thereby modulating the incident carrier provided by the reader. The reader observes this on-off backscattering pattern and can decode the signal.

Backscatter Tag Architecture

Since backscatter tags only need to reflect the incident carrier signal, their design is exceedingly simple. Figure 2(a) and (b) show how a backscatter tag transmits and receives data. Its transmitter end is simply an RF transistor that can be modulated by a simple low-frequency clock that operates at a few tens of kHz for ASK modulation, and around several MHz for FSK modulation. At the receiver end, the tag uses an envelope detector that comprises of a comparator and passive resistor/capacitor components and rectifying diode.

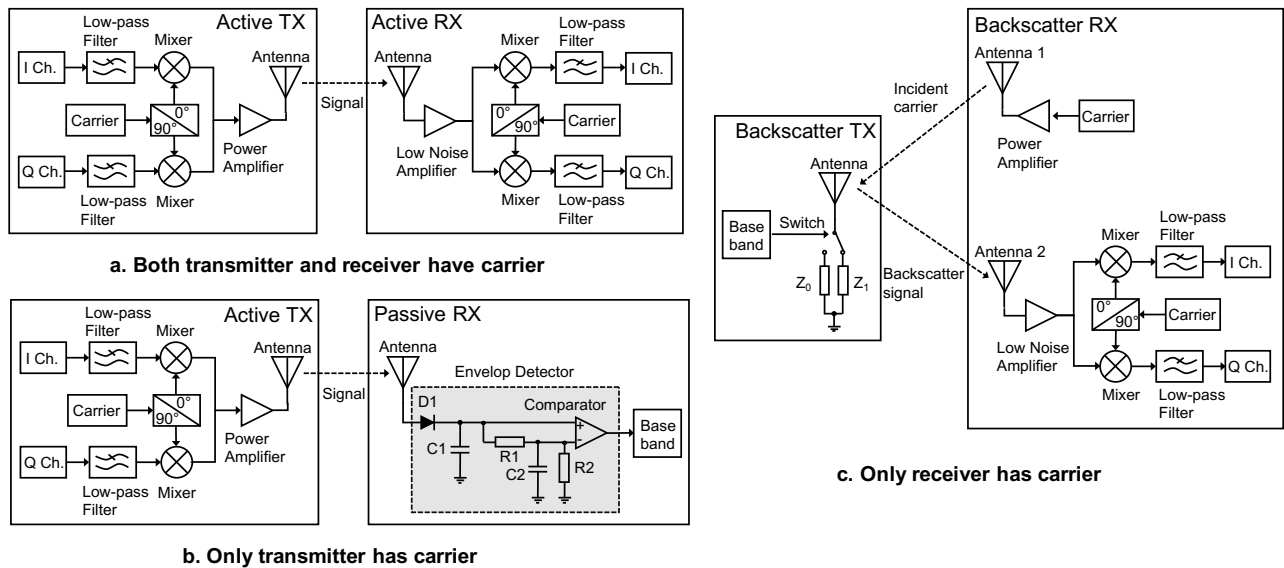


Figure 2: Three architectures with different carrier placement.

Table 2: Power consumption and cost of commercial readers

Model	Total Power consumption	Est. RX Power consumption	Cost
AS3993[2]	0.64W@17dBm	0.25W	\$397
AS3992[1]	0.73W@20dBm	0.26W	\$303
R2000[12]	1W@12dBm	0.88W	\$419
R1000[11]	1W@12dBm	0.95W	\$500
M6e[18]	4.2W@17dBm	4.0W	\$398
M6micro[19]	2.5W@23dBm	2.5W	\$285

The detector itself consumes zero power since its a passive circuit, making it ideal for tags.

Backscatter Reader Architecture

In contrast to tags, backscatter readers are fairly complicated systems that are bulky and consume a lot of power. The reader-side power consumption for commercially available RFID reader chips is provided in Table 2, and we can see that it ranges from several hundred milliwatts to a few watts. To understand why, we need to explain more about how readers work and what makes them complex.

The complexity of backscatter readers arises primarily from the methods that they use to deal with self-interference — the reader generates the carrier for the tag, but the strong self-interference from the carrier can overwhelm the weak backscattered signal.

How do readers manage self-interference: Commercial readers use a combination of methods to deal with self-interference including: 1) isolation of the carrier from receiver, 2) attenuation of self-interference with RF cancellation, and 3) separation of the self-interference signal by converting it into DC voltage. Isolation methods use either multiple antennas

or RF devices called directional couplers [44] to try to isolate the carrier [40]. RF cancellation is another widely used technique, wherein the reader generates a cancellation signal and adds it to the received signal. Finally, a third method is to convert the signal including interference to baseband directly called Zero-IF. Here, the system uses a mixer with the local oscillator working at exactly the carrier frequency (and hence self-interference frequency), and converts the signal to baseband in a single frequency conversion.

But these techniques do not come cheap. Directional couplers tend to introduce insertion loss, and increases the transmit power if user want to maintain the same output power. RF cancellation requires an accurate estimate of the amplitude and phase of the interference signal, which in turn requires frequent channel measurements and extensive communication. In addition, the cancellation signal needs to be generated by the receiver, which consumes tens of milliwatts of power. Direct conversion to baseband also requires carrier generation, mixing, and various filters which consumes roughly 60mW of power.

3. BRAIDIO DESIGN

Our goal in Braidio is to design a radio that is minimalist, integrated, and low-power such that it is practical on battery-powered devices. To do so, the primary issue that we need to deal with is the high power consumption when operating in backscatter mode.

3.1 Design rationale and key insights

Can we do better than commercial readers in terms of power consumption? When considering this question, we need to be realistic; if we wish to dramatically reduce power consumption, we have to be willing to sacrifice some sensitivity. We simply cannot afford to use a combination of high transmit power, RF cancellation and Zero-IF methods

used by commercial readers — in fact, even using any one of them might take us over our target power budget. This might seem like a major downside, but let us look at what is the consequence of reduced sensitivity.

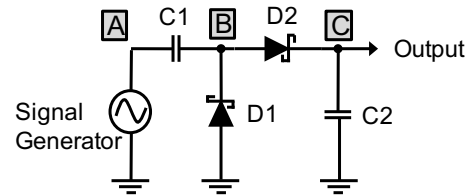
On a commercial reader, reduced sensitivity means inability to read RFID tags at desired read ranges. This would be problematic in real-world scenarios such as supply chain inventory control where these readers are used. When viewed from this lens, it is understandable why readers over-provision to ensure high sensitivity while sacrificing power efficiency. The energy budget is also not a huge constraint since even hand-held RFID readers are intended to be the size of a power-drill, not the size of a smartphone or wristband.

But reduced sensitivity in Braidio has entirely different consequences. For Braidio, a loss of sensitivity means that we have to switch back to active mode from backscatter mode. This means higher power consumption at the transmitter end, which is an inconvenience but not a show-stopper. In other words, Braidio has a safety net when backscatter sensitivity becomes a problem, and can easily fallback to the more reliable, but perhaps less desirable, active mode. This difference has huge consequences since it means that we have room to explore more unconventional designs that focus primarily on reducing power consumption while sacrificing some sensitivity in the process.

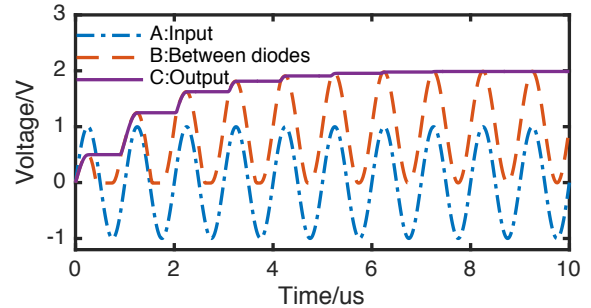
This leads us to our key idea, which is to leverage a simple envelope detector based receiver and use it as a building block for passive self-interference cancellation. The envelope detector is an extremely simple receiver circuit and is also commonly used on backscatter tags to receive data from a reader. This detector can be turned into a passive receiver that is capable of self-interference rejection if we combine it with a high-pass filter. If the self-interference channel is stationary, then self-interference presents as a DC offset at the output, which would not affect backscatter signal reception. Even if the self-interference channel is dynamic, its coherence time is typically in the order of milliseconds [26], which means that it creates low frequency components less than 1kHz. These low frequency components can be easily removed by high pass filtering.

This observation opens the door for an end-to-end integrated version of Braidio that is no more complex than a typical active radio combined with a small amount of extra circuitry that is effectively similar to the components needed to design a passive tag! With just this combination of parts, we may be able to design a minimalist, low-complexity, and low-power radio that is capable of operating in both active and passive modes.

Our design has substantial implications in practice. First, it means that the bill-of-materials cost can be kept low since we only add a tag’s worth of components to an active radio like BLE. This is important for radios that are intended for low-cost devices such as mobile phones and wearables (e.g. the Nordic nRF51822 and TI CC2540 cost \$2.5 in volume). Second, lower complexity also means less real-estate needed on the device, which is another major consideration on small form-factor portable devices. Third, by integrating the active and passive components into a single radio with



(a) A single stage RF charge pump.



(b) TINA simulation of charge pump.

Figure 3: Circuit diagram and simulated output of RF charge pump.

shared modules, we can switch between the modes easier since components need to be turned off and on fewer times.

While this high-level idea guides our design, many issues need to be dealt with to make it practical. We now discuss these issues.

3.2 Low-power Backscatter Reader RX

Let us consider the core idea in a bit more detail. The solution we discussed is to use a passive receiver at the reader side based on a RF charge pump [33]. This receiver relies on several stages of a diode-capacitor configuration that can boost the voltage of a weak signal received at the RF front end. At the same time, the configuration blocks the large but relatively constant carrier self-interference signal from passing through.

The circuit and working mechanism is shown in Figure 3. The charge pump circuit extracts the envelope of the dynamic RF signal and converts it into DC voltage. Given a sine wave signal with amplitude of 1V, it can generate 2V DC voltage at the output as shown in Figure 3(b).

This design has two benefits in terms of performance. The main advantage of a passive receiver is the ultra low power consumption. The receiver is entirely passive and is excited by incident RF signal so it requires no external power supply and consumes near-zero power draw. This reduces the overall power consumption of the backscatter subsystem to levels that are acceptable on mobile platforms. From a performance standpoint, a passive receiver also tackles the self-interference problem because it convert self-interference to DC directly, and can be separated out from useful signal in frequency domain. This makes it possible to extract out the weak backscatter signal despite there being a large self-interference signal from the carrier transmitter.

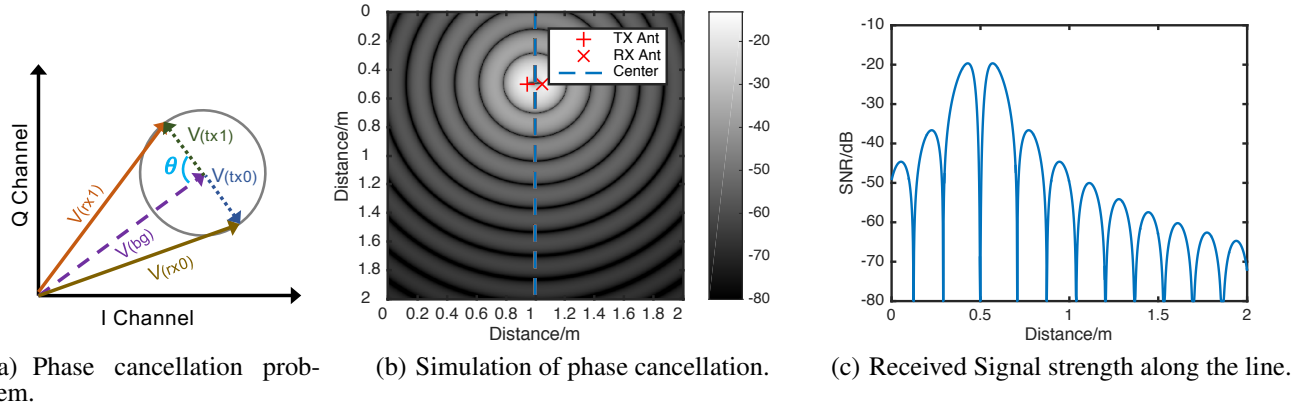


Figure 4: Illustration of the phase cancellation problem.

However, there are several additional concerns that need to be addressed for a passive receiver to be practical. From a sensitivity perspective, the main issue is that the backscatter signal is quite weak, and the output from the charge pump may be insufficient for robust decoding. This means that we may need additional active circuits beyond the passive receiver to ensure reception of weak backscattered signals. From a robustness perspective, the issue is that an envelope-based detector is incoherent i.e. it is not sensitive to carrier phase unlike the coherent detectors on RFID readers. This means that we have to deal with phase cancellation issues wherein the amplitude of the signal extracted by the non-coherent detector can remain unchanged even though the backscatter transmitter is actually changing its transistor state. Finally from a channel selectivity perspective, the issue is that a passive envelope detector is not selective in terms of which channel it tunes into, and just looks at the energy in a wide bandwidth.

We now look at how we can tackle these three issues.

Improving sensitivity via instrumental amplifier: The output of the Dickson RF charge pump has very low voltage, so it can lead to low receiver sensitivity. Typically, the signal amplitude has to be at least several mV [14, 20] for the comparator to generate the correct output, resulting in a sensitivity of around -40dBm. In principle, a charge pump can boost the signal by $2N$ times where N is the number of stages of charge pump. But this is far from enough to bridge the gap to commercial, active receiver ICs, which is in the order of -80dBm. To solve this problem, we added an instrumental amplifier between the output of charge pump and the input of comparator. A charge pump boosts voltage but it also increases the output impedance significantly since it is passive and the output power cannot be larger than input power. Thus the circuit has to be tuned carefully and the amplifier has to be high impedance and low input capacitance, otherwise the signal will be greatly reduced.

Antenna diversity to address phase cancellation: Since an envelope-based receiver is non-coherent and insensitive to phase, it can suffer from the phase cancellation problem.

This refers to a particular situation where the signal from the backscatter transmitter is orthogonal to the background signal (including self-interference), as shown in Figure 4(a). The signal amplitude at the envelope detector is $A = ||\vec{V}_{rx1} - \vec{V}_{rx0}||$. Assuming that $\vec{V}_{tx0} = -\vec{V}_{tx1}$ we could have $A = 2\cos(\theta)||\vec{V}_{tx0}||$. When θ is close to $\frac{\pi}{2}$, the signal amplitude will become very weak. If $\theta = \frac{\pi}{2}$, changes in the transistor state at the backscatter transmitter will not change the signal amplitude at the receiver, and only changes the phase. Since an envelope detector cannot detect phase, it will see no change in the received waveform and will be unable to decode the signal.

Figure 4(b) shows a visualization of signal strength when we place a transmit antenna at $X=0.95m$, $Y=0.5m$ and receive antenna at $X=1.05m$, $Y=0.5m$. The darker the color, the weaker the received signal. We see that in addition to free space path loss [40] which is proportional to the square of distance, we can observe dark regions which are very close to the transmitter and receiver due to phase cancellation. Figure 4(c) shows the received signal strength along the line shown in Figure 4(b). We can see that there are null points with very low SNR quite close to the devices with $Y=0.5m$, which would result in high bit error rate.

The technique that we use to combat this issue is antenna diversity. This is a widely used technique to tackle destructive multi-path interference [22, 27]. If signals from all paths are destructive at one antenna, the hope is that a second antenna will experience sufficiently different channel conditions to provide a better SNR. A graphical illustration is shown in figure 5. Assuming that we have two received antennas with different distance to the transmit antenna, we can expect to have two different background signal vectors $-\vec{V}_{bgch1}$ and \vec{V}_{bgch2} . Similarly, the received signal amplitude of antenna 1 is determined by θ_1 and the path loss, and θ_2 and path loss determine the received signal strength. If $\cos(\theta_1)$ is close to zero, we try to decode signal from receive antenna 2 assuming that $\cos(\theta_2)$ is large, so signal strength from antenna 2 is stronger.

Figure 6 shows a microbenchmark comparing the SNR

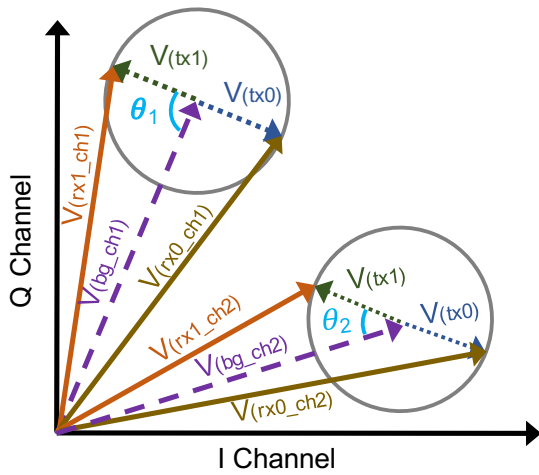


Figure 5: Illustration to show how we combat phase cancellation with 2-antenna diversity

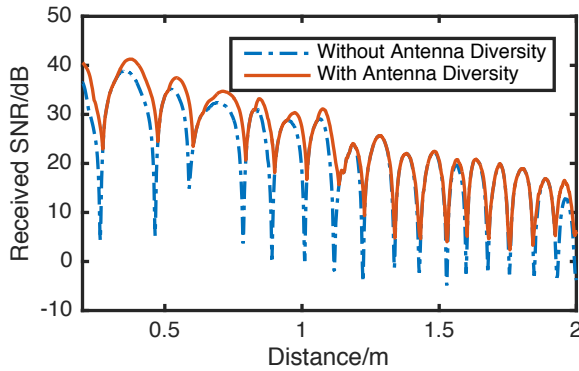


Figure 6: Effect of antenna diversity on SNR. Antenna diversity mitigates effect of phase cancellation.

difference with and without antenna diversity. From the figure we can observe that without antenna diversity, the SNR can drop from about 30dB to around 0dB, causing errors in detection. With antenna diversity, the SNR at null points are still higher than 5dB, enabling correct detection.

Frequency selectivity: Another issue we need to address is that a simple envelope detector is not frequency selective. Out of band interference coming from a cellphone or WiFi router can trigger the envelope detector circuit resulting in poor reception. We solve this problem by putting a Sound Acoustic Wave (SAW) filter at the radio front-end to ensure that the envelope detector only receives signal within the intended license-free band. SAW filters are passive components which do not incur additional power consumption.

Summary: Commercial Reader v.s. Braidio

We conclude with a brief summary of the many differences between our design and the design used in a commercial R-FID reader, summarized in Table 3. At a high level, our goal is to reduce power and complexity while not sacrific-

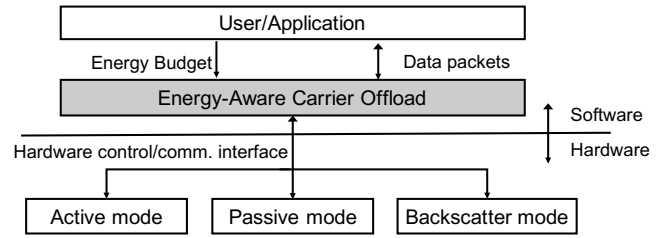


Figure 7: Energy aware carrier offload layer

ing much performance. Our key differences are that a) we eliminate the use of a mixer and low-pass filter and instead use a passive SAW filter, b) we eliminate the Low Noise Amplifier, the IF filter, and signal processing components and instead use charge pump and amplifier on the resulting signal, and c) we eliminate the need for an IQ-based orthogonal receiver and instead simply use an antenna switching scheme.

4. ENERGY-AWARE CARRIER OFFLOAD

At a high level, Braidio offers three modes of operation (named after the receiver states). The first is the *active mode* where both transmitter and receiver have carrier, and corresponds to the case when Braidio behaves like an active radio. The power consumption in this mode is mostly symmetric, with some wiggle room by changing transmit power level. The second is the *passive receiver mode* where only transmitter has carrier, and the receiver uses a passive envelope detector to save power. This mode of operation is not one we sought out to design, but is an interesting option that we enable through our architecture. The power consumption in this mode is asymmetric, with the transmitter consuming as much as an active radio but the receiver operating like a passive radio and consuming minimal power. The third mode is the *backscatter mode* where only receiver has a carrier, which is equivalent to the backscatter scenario where the reader does most of the work. This mode is the one that allows the transmitter to offload the carrier to the receiving end-point in order to save energy. Here, the data receiver consumes more power since it is transmitting the carrier and also doing the work to cancel self-interference and decoding the signal as discussed earlier. But the data transmitter is a simple backscatter tag which is extremely power efficient.

Our goal in this section is to design a layer above the raw hardware that enables dynamic carrier offload, i.e. that switches between the three modes in proportion to the energy availability at the two end-points, as shown in Figure 7. For example, consider the case where in mode (a), both end-points generate the carrier and each consumes 50mW, and in mode (b) one end-point generates the carrier and consumes 120mW with the other end-point consuming 10μW. Let the ratio of available energy on two devices d_1 and d_2 be 10:1. To operate in an energy-aware manner, these devices can multiplex between the two radio modes and use mode (a) 90.9% of the time and mode (b) 9.1% of the time such that d_1 consumes 109mW and d_2 consumes 10.9mW.

Table 3: A comparison of commercial reader and Braidio

	Commercial Reader	Braidio
Phase cancellation	IQ based orthogonal receiver Pros: robust, accurate signal amplitude measurement Cons: two set of mixers, filters, IF amplifier. High power consumption	Antenna diversity, spatially separated Pros: passive, lower power consumption Cons: can not eliminate null points completely
Signal Amplification	RF LNA, IF amplifier and digital signal processing Pros: better sensitivity Cons: high power consumption	Boost signal with charge pump and amplifier Pros: lower power consumption Cons: lower sensitivity
Frequency selection	Mixer and low pass filter Pros: better frequency selection Cons: high power consumption	SAW filter eliminate out-of band signal Pros: zero power consumption Cons: may be interfered by in-band signal

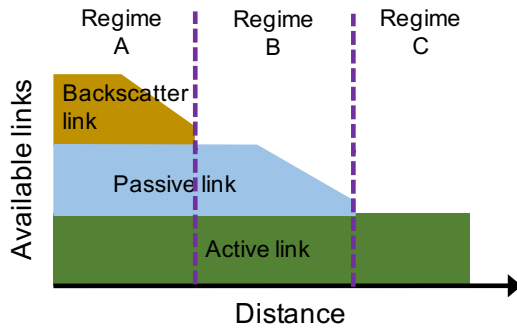


Figure 8: Three operating regimes of Braidio

But the above description over-simplifies the problem. The three modes are not identical in performance since they have differences in hardware, path loss, reflection loss, etc. As a result, they have different signal-to-noise ratios which translates into differences in range and throughput. Intuitively, Braidio in active mode should offer more throughput and range compared to the passive receiver mode, which in turn should have higher throughput and range than the backscatter mode. Thus, an energy-aware carrier offload method needs to consider which modes are available at any given time, and what performance they offer.

4.1 Braidio Operating Region

Braidio operates in three distinct regimes as illustrated in Figure 8. Regime A allows us to move the carrier to either end-point depending on the energy availability, and presents the maximum flexibility in the use of the three operating modes of Braidio. When devices operate in this regime, we can enable power-proportional carrier offload, where the end-point with more energy availability takes a lions share of the overall cost of communication. In Regime B, the transmitter has to generate a carrier since the backscatter mode no longer works. However, if the transmitter has more energy than the receiver, it is possible to operate for the receiver to switch its carrier off and operate in passive receiver mode. In Regime C, the transmitter and receiver have to generate the carrier since the SNR is too low for the receiver to decode via a passive envelope detector.

4.2 Carrier Offload Algorithm

The carrier offload algorithm is the decision engine that determines which mode should be used. Figure 9 shows a useful way to visualize the options available to a Braidio radio at any given time. The x-axis is the efficiency (in bits/joule) for the transmitter, and the y-axis is the efficiency (in bits/joule) for the receiver. Let us first look at the three corners of the triangle, labeled A, B, and C. These correspond to the transmitter–receiver efficiencies for each of the three operating modes. The active mode (point A) is somewhat symmetric in efficiency at the two endpoints; the passive receiver mode (point B) has higher efficiency for the receiver than transmitter; and the backscatter mode (point C) has higher efficiency for the transmitter because all the overhead is shifted to the receiver.

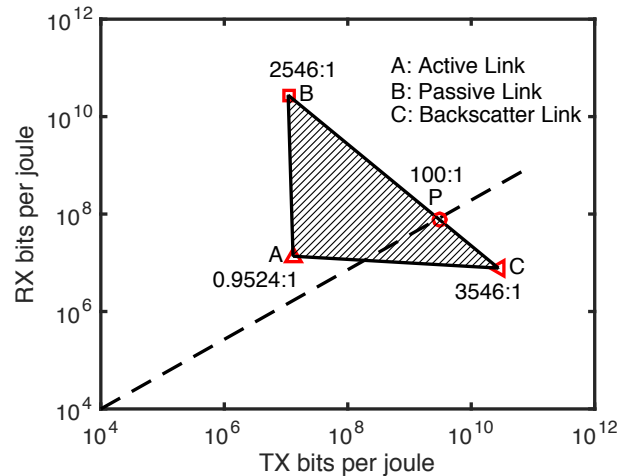


Figure 9: Dynamic range of power assignment of Braidio in terms of transmitter to receiver energy efficiency ratio.

By multiplexing across these modes, different power ratios can be achieved as shown in the shaded region in the figure ($\triangle ABC$). While the shaded regions represent the feasible transmitter–receiver power ratios, note that the different modes of operation also have different overall efficiencies (i.e. the cumulative transmitter + receiver efficiency). As a result, not all the feasible operating points may be

desirable. The optimal operating points in terms of overall energy efficiency would lie on line BC of the triangle since this has the best cumulative efficiency. So, for example, take the case of a transmitter–receiver pair who have an energy ratio of 100:1. To operate in a power-proportional manner, they would need to pick a point on the dotted line in the figure. The point on that line that maximizes the number of bits they can transfer while operating power-proportionally is the point P on line BC.

This leads us to the working of the carrier offload algorithm. Initially, the transmitter and receiver exchange information about their battery status using the active radio. Given this information, they need to decide what operating modes to use, and what fraction of the time to use the mode to achieve power-proportional operation. The possible operating modes that the two end-points can use for communication are limited by two factors: a) the battery status of the end-points and b) the SNR of the different links.

Such considerations are taken into account in a pruning step that limits the space of possible options. The two end-points use probe packets over the two links to determine the SNR and bitrate parameters, and exchange this information. At this point, each end-point has information about a) the energy-level at the two end-points, and b) the power efficiency on the transmitter and receiver side for the highest bitrate that can be supported for each of the three modes of operation (measured in bits per joule).

Let E_1 and E_2 are the energy levels at the two ends, and T_i means that in mode i , the transmitter consumes T_i joules to send one bit of data to a receiver, and R_i is the corresponding cost to receive one bit of data. The carrier offload algorithm tries to find the optimal strategy in terms of what fraction of time to transmit in each mode p_i such that we can be power-proportional in the energy consumed at the two ends. This can be formulated as:

$$\begin{aligned} & \underset{p_1, p_2, p_3}{\text{minimize}} && \sum_{i=1}^3 p_i (T_i + R_i) \\ & \text{subject to} && \sum_{i=1}^3 p_i = 1, \\ & && \frac{\sum_{i=1}^3 p_i T_i}{\sum_{i=1}^3 p_i R_i} = \frac{E_1}{E_2}, \end{aligned} \quad (1)$$

Once the fraction of time to operate each mode is determined, Braidio simply switches between the modes after a certain number of packets to achieve that proportion. For example, if $p_1 = 0.5$, $p_2 = 0.25$, $p_3 = 0.25$ then a possible sequence of modes could be Active-Active-Passive-Backscatter (repeated).

Of course, the wireless link is dynamic, particularly in a mobile environment. Braidio simply falls back to the active mode if the current operating mode is performing poorly. Thus, when in passive receiver mode, the receiver switches to active receiver mode when it observes that the SNR is

too low. When the backscatter mode performs poorly, the receiver turns off the carrier, which implicitly informs the transmitter that it needs to turn on the carrier. Switching modes in the other direction is easy too — when SNR is high in active mode, the system can either switch into passive receiver mode or backscatter mode depending on the direction of energy asymmetry. Braidio also periodically re-computes the ratio of using different modes depending on observed dynamics. If SNR or loss rate changes significantly, it re-calculates the ratio according to Equation 1.

5. IMPLEMENTATION

The design of Braidio has evolved over several hardware iterations that we have used to measure and identify problems. Our first version of Braidio was designed entirely from off-the-shelf components — a TI CC2541 Bluetooth/BLE radio, a low-power UHF reader IC (AS3993 [2]), and a Moo Backscatter tag. Our measurements of this platform were highly unsatisfactory from a power perspective, which in turn led to further revisions. Our second version of Braidio was designed to further improve power draw. This version used a directional coupler for isolation, and a Zero-IF method to directly convert the signal to baseband. Our measurements with this platform were also unsatisfactory since the reader by itself combined more than 240mW of power. Our third version of Braidio is the one that we use in this paper and describe further.

Modular design: As we proceeded through the evolution of Braidio, we also made our system more modular since this helped us re-use hardware components when we only needed to change a part of the design rather than the entire radio. It also helped with isolate errors and simplify debugging.

Figure 10 shows the final version of the hardware that we use in this paper. It consist of a microcontroller and active radio on the back of PCB, a passive receiver module and baseband amplification circuit, an antenna switching module, three chip antennas and SAW filters. We connect these components using U.FL. cables. The board also has a Bluetooth module on the back acting as the active transceiver. Note that these components can be further integrated into an ASIC version of Braidio. Both the modules and main board are made with 4 layer PCB process for better performance. RF traces are designed under controlled impedance using coplanar wave guide calculator [51]. A detailed description of each hardware module is shown in Table 4.

Implementation challenges: We faced many low-level implementation challenges. One major issue that we dealt with was the limited size of Braidio. Braidio is designed to work with mobile, even wearable devices, so form factor is an important issue. Therefore, instead of using dipole antenna which measured more than 15cm (used on Moo and WIS-P), we used chip antennas to keep Braidio small. This design choice necessitated that we improve sensitivity of receiver. In addition, having multiple antennas for antenna diversity on a small PCB board required careful placement to deliver good performance. We also used U.FL. connectors instead of SMA to reduce size. Finally, another challenge we faced

Table 4: Description of hardware modules in Braidio

Module	Model	Description
Controller	ATMEGA 328P	Arduino-compatible; consumes only 2mA@8MHz
Carrier Emitter	SI4432	125mW@13dBm
Passive Receiver	Moo [53]/WISP [47]	Reduced C_s and C_p to improve bitrate
Baseband Amplifier	INA2331	Low input capacitance - 1.8pF
Antenna Switch	SKY13267	SPDT; less than 10uW power consumption
Chip Antenna	ANT1204LL05R	Two antennas separated by 1/8 wavelength, only 12mm in length each
SAW Filter	SF2049E	50dB suppression at 800MHz band; >30dB suppression at 2.4GHz band
Active Radio	SPBT2632C2A	small/low power while providing Bluetooth abstraction over serial interface

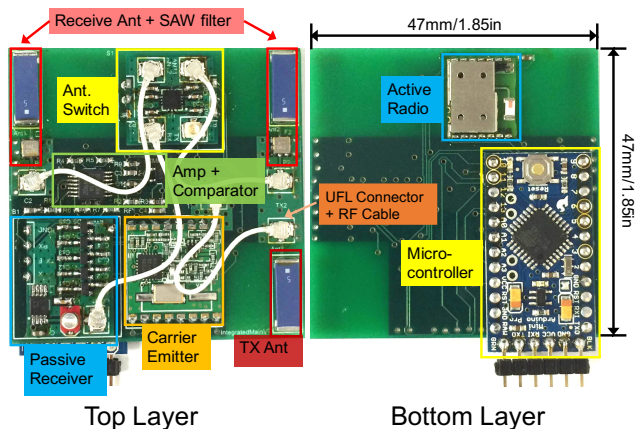


Figure 10: Hardware implementation of Braidio

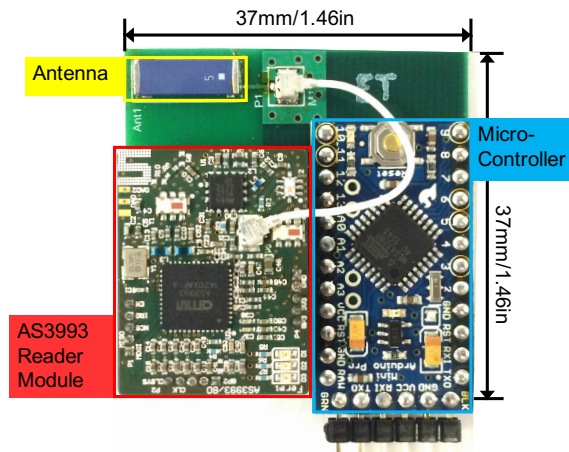


Figure 11: AS3993 reader test board

is tuning the RF circuits which required careful matching to avoid reflection loss and careful component placement and PCB wiring.

RFID Reader Board: In order to have a good baseline to compare our results against, we use the AS3993 Fermi reader from AMS [2]. We choose AS3993 because it is among the lowest power commercial readers. In addition, it supports direct mode and makes it possible to implement customized Backscatter protocols. We developed an adapter board to connect it to an Arduino, as shown in Figure 11.

6. EVALUATION

We now turn to an end-to-end evaluation of Braidio. We start with a full empirical characterization, and use this characterization to design a simulator. Our simulator allows us to understand performance improvements of using Braidio when devices with different energy budgets for communication.

6.1 Braidio v.s. commercial reader

We first evaluate the performance of Braidio against the commercial AS3993 reader. Figure 12 shows the bit error rate of Braidio and commercial reader at 100kbps. Braidio has an operational distance of 1.8m, whereas the commercial reader operates up to 3m. So, as expected, our design has about 40% lower range than a commercial reader. How-

ever, the commercial reader also consumes 640mW while Braidio consumes only 129mW. Thus, Braidio is about $5\times$ as efficient as the commercial reader. Note that the AS3993 is the lowest power reader that we found, and gains are even larger against other readers (Table 2). The experiment is carried out in an empty, $6m \times 6m$ room. We clear the area to minimize the effect of environmental reflections.

6.2 Characterizing Braidio Performance

In this experiment we characterize the performance of Braidio using two metrics: a) bit error rates at different distances, and b) transmit and receive energy-efficiency in bits/joule. Our goal is to identify the practical boundaries between the three regimes of operation outlined in §4.1, and the performance that Braidio can achieve in these different regimes.

BER vs Distance: Figure 13 shows the bit error rate (BER) at increasing distances for the operating modes at different bitrates. The active mode operates well beyond 6 meters (which is the maximum distance we can have in our setting), so we do not show it in the plot. As expected, the backscatter mode has the lowest range. At 1Mbps, backscatter has a range of slightly less than a meter (for $BER < 0.01$), but the range increases to 1.8m at 100kbps and to 2.4m at 10kbps. The passive receiver mode operates at up to 3.9 meters at 1Mbps, and increases to 4.2m at 100kbps and 5.1m at 10kbps.

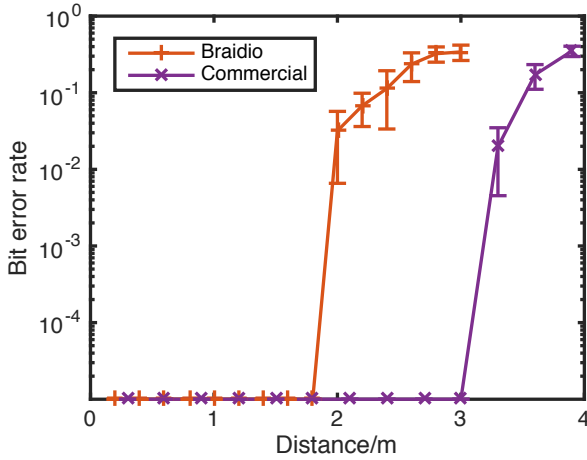


Figure 12: Bit error rate for Braidio and commercial reader at 100kbps.

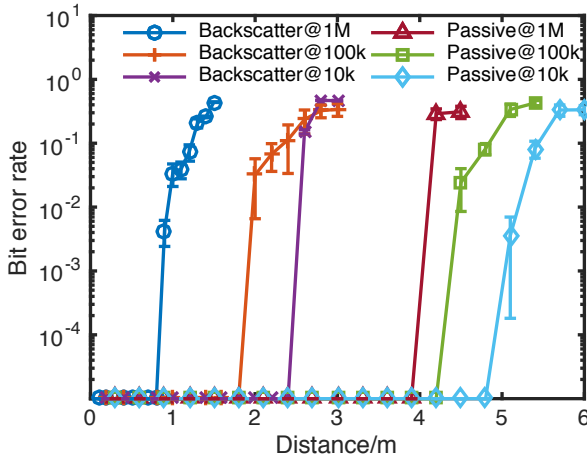


Figure 13: Bit error rate over distance for backscatter and passive receiver modes at different bitrates.

Transmitter-Receiver Efficiency: We now turn to the achievable region in terms of the TX:RX power ratios offered by two Braidio radios that are separated by different distances. Figure 14 shows how the supported power ratios change as separation increases from 0.3m to 6m (using the representation in Figure 9). Each triangle refers to the achievable region at a particular distance between the transmitter and receiver. The shaded region in each triangle represents the possible operating points if we multiplexed between the different modes. The two lines on the left represent cases where the backscatter mode no longer operates, so we only have the active and passive receiver modes, making the possible operating points a line.

At 0.3m, all the links are available at the highest bitrate. Braidio operates primarily in passive receiver or backscatter mode at this distance, and switches between them to achieve different power ratios. The dynamic range that can be supported by Braidio is largest at this range — it can support

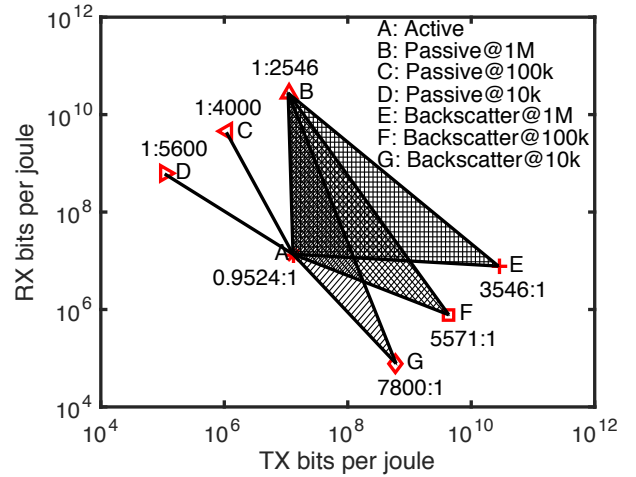


Figure 14: Energy efficiency and dynamic range of Braidio at different distances and bit rates

Table 5: Switching overhead in different modes

Mode	TX	RX
Active [8]	$1.05 \times 10^{-9} \text{Wh}$	$1.01 \times 10^{-9} \text{Wh}$
Passive	$1.72 \times 10^{-9} \text{Wh}$	$4.40 \times 10^{-12} \text{Wh}$
Backscatter	$8.58 \times 10^{-8} \text{Wh}$	$1.10 \times 10^{-11} \text{Wh}$

TX:RX power ratios between 1:2546 and 3546:1, i.e. a seven orders of magnitude span!

As the distance increases, the backscatter link switches from 1Mbps to 100kbps at 0.9m and finally to 10kbps at 1.8m. This drops the efficiency of the transmitter and receiver, and the triangle becomes increasingly obtuse. In other words, Braidio can still offer asymmetric power modes, but they just become a bit more expensive in terms of bits/joule at the transmitter and receiver. So, the overall gains reduce as the separation increases.

Beyond 2.4m, the backscatter mode becomes unavailable. At this point, only the active and passive receiver modes are viable, so the operating region is a line between these modes. Note that since backscatter is the only mode that offloads the carrier to the receiver, the nature of asymmetry that is supported after 2.6m is favors the receiver rather than transmitter. As distance increases further, the passive receiver mode also drops in supported bitrate, until after 4.5m, only the active mode is available and the feasible region shrinks to a single point.

Switching overhead: We also characterized the switching overhead of Braidio in different modes. The result is shown in Table 5. Notice that for the Backscatter case, we use the worse scenario, i.e. the link speed is only 10kbps. Experimental results indicate that switching overhead is negligible in all modes.

6.3 Braidio for Portables

In this section we look at how the ability to operate in an asymmetric manner can be useful across a range of portable devices with different battery capacities. To understand this, we design a simulator that simulates link behavior based on

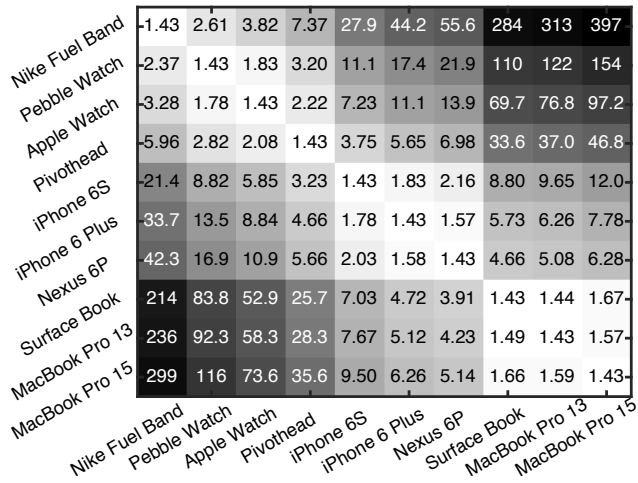


Figure 15: Performance gain of Braidio over Bluetooth when device on horizontal axis transmits to device on the vertical axis

the above described experimental characterization, and outputs the simulated performance given as input the energy levels of two end points and the traffic pattern between them. Our simulator includes a full implementation of the energy-aware carrier offload algorithm described in §4. Note that the results only consider the communication subsystem, and real-world performance would depend on other factors as well. But the goal is to illustrate the potential benefits if communication were the power bottleneck.

Our experiments in this section cover communication between devices ranging from wrist-worn fitness bands with small batteries to laptop-class devices with much larger batteries. We report the results as a matrix where each cell corresponds to the *performance gains over a baseline method* i.e. if the device on the x co-ordinate of the cell were communicating with the device on the y co-ordinate of the cell using Braidio vs a baseline method, how many more total bits can be communicated between the transmitter and receiver when we use Braidio. The shading of the cells in the matrix corresponds to the magnitude of the gains (larger gains means more darkly shaded cells).

Scenario 1: Different battery sizes

Figure 15 shows the result when a transmitter (x axis) transmits data continuously to a receiver (y-axis). In this experiment, we assume that the transmitter and receiver are less than one meter apart, so all modes can operate at their peak bitrate. Both end points start with a full battery, and we record the number of bits transmitted until either the transmitter or receiver runs out of battery.

The figure shows that Braidio outperforms Bluetooth by up to 397×. The maximum gains correspond to the scenarios where a device with a small battery is transmitting to a device with a large battery since backscatter mode can be leveraged, or when a device with large battery transmits to a device with small battery in which case the passive receiver can be leveraged. In reality, some devices gener-

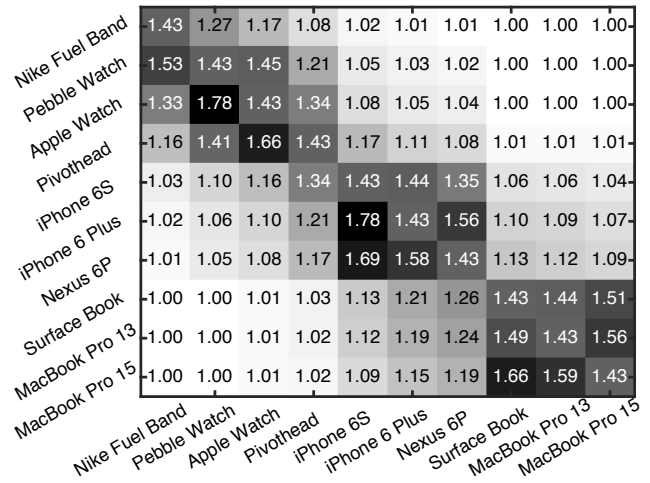


Figure 16: Performance gain of Braidio over the best of the three modes. Data transmission is from the device on the horizontal axis to the one on the vertical axis.

ate more data than others, so the more data-rich devices are the ones most likely to benefit from Braidio. For example, the Pivothead is a device that has an outward-facing camera and streams at 30fps (similar to GoPro and Google Glass), and Braidio improves lifetime by 35× for communication between this device and a laptop.

Curiously, the diagonal lines from upper left to bottom right in Figure 15 show the performance gain of Braidio even when the energy ratio is 1:1 i.e. both transmitter and receiver have the same amount of energy. While this may seem counter-intuitive, the gains occur because Braidio does not turn on the carrier on both ends unlike an active radio. So, Bluetooth turns on the carrier on both ends whereas Braidio turns on the carrier at one of the ends but ends up using higher power at that end compared to Bluetooth. Even so, Braidio can get 43% performance improvement over a commercial radios since the transceiver on each side only need to generate the carrier for half of the time.

Braidio v.s. the best of the operating modes: One unanswered question in the above experiment is whether the two devices end up using only one of the operating modes throughout the experiment, or whether they switch between the different modes as the amount of energy at the end points dwindle. To understand the benefits of switching between the different Braidio modes, we look at the total bits communicated if one of the three modes were exclusively used, and then compare Braidio against the best of these three modes in isolation. The results are shown in Figure 16.

The results show that when the battery levels are highly asymmetric, Braidio almost exclusively uses a single mode, but when the devices have somewhat similar battery levels, it switches between the modes. Switching provides up to 78% improvement across the scenarios tested. In reality, the energy levels of mobile and wearable devices varies significantly depending on charging and usage patterns, so switching between modes is necessary to deal with these dynamics.

Nike Fuel Band	-1.43	2.45	3.51	6.63	24.7	39.1	49.1	251	276	350
Pebble Watch	-2.57	1.43	1.76	2.97	9.98	15.5	19.4	97.7	107	136
Apple Watch	-3.68	1.85	1.43	2.11	6.51	10.0	12.4	61.6	67.9	85.8
Pivothead	-6.97	3.12	2.21	1.43	3.45	5.12	6.29	29.8	32.8	41.4
iPhone 6S	-25.9	10.4	6.83	3.62	1.43	1.77	2.05	7.89	8.64	10.7
iPhone 6 Plus	41.0	16.3	10.5	5.37	1.85	1.43	1.54	5.19	5.65	6.99
Nexus 6P	51.6	20.4	13.0	6.60	2.16	1.61	1.43	4.24	4.61	5.68
Surface Book	263	102	64.7	31.3	8.29	5.44	4.46	1.43	1.43	1.63
MacBook Pro 13	290	113	71.3	34.4	9.07	5.94	4.85	1.50	1.43	1.54
MacBook Pro 15	368	143	90.1	43.4	11.3	7.34	5.96	1.71	1.62	1.43
Nike Fuel Band										
Pebble Watch										
Apple Watch										
Pivothead										
iPhone 6S										
iPhone 6 Plus										
Nexus 6P										
Surface Book										
MacBook Pro 13										
MacBook Pro 15										

Figure 17: Performance gain of Braidio over Bluetooth for bi-directional data transmissions between two devices

Scenario 2: Bi-directional communication

In Scenario 1, we assumed that traffic was one way between the device on the x axis to the device on the y axis. But what if the communication was bi-directional, for example, when a device is both a sensor as well as a display device (like Google Glass and HMDs). We now study the effect of bi-directional data transfer i.e., when the transmitter and receiver switch roles after send a certain amount of packets. Equal amount of data is transmitted in both directions. We compare against Bluetooth as baseline. Experimental results are shown in Figure 17.

The results are a bit better than the unidirectional case. This is because in highly asymmetric scenarios, the device with less energy budget is able to use the backscatter mode when communicating and the passive receiver mode when receiving, which increases the benefits. When devices are somewhat symmetric, the benefit is limited.

Scenario 3: Increasing distance

So far, we have assumed that the transmitter and receiver are a short distance apart so that all modes have roughly equal throughput. Let's now explore whether the performance benefits of Braidio remain as distance increases. We choose three pairs of devices to study how the benefits evolve as distance increases. The results are shown in Figure 18.

The performance of Braidio at short distances is extremely strong since the asymmetric modes are viable and efficient. When the bitrate of the backscatter mode drops, so do the benefits we can get with Braidio although we can still get more than $10\times$ improvement compared to Bluetooth. Finally, at 2.4m, we transition out of the zone where backscatter communication can work. so we can only use the active and passive receiver modes. So, the benefits are only available in cases where a device with a large energy budget is transmitting to a device with a small energy budget, as shown in the top right part of the matrix in Figure 15. We don't show the result with distance longer than 6m because only the active

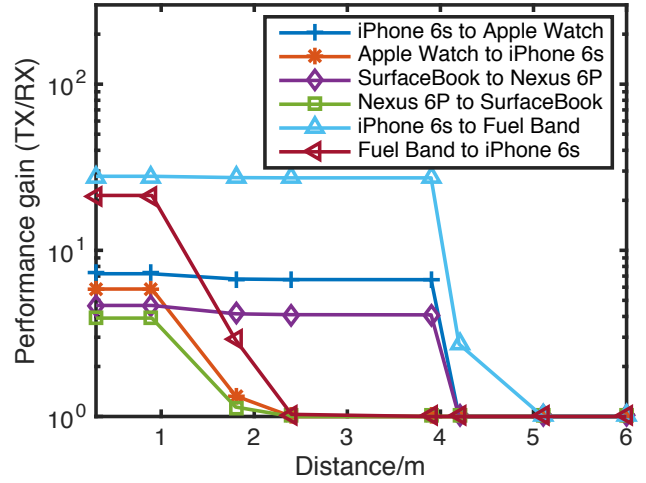


Figure 18: Performance gain of Braidio over Bluetooth for transmission over different distances.

mode works, so the performance of Braidio is identical to Bluetooth.

7. RELATED WORK

The problem of low-power wireless communication has seen decades of research. Of particular note is methods that use two radios; for example, [23, 35, 42] employ multiple wireless interfaces such as WiFi and Bluetooth to achieve better energy efficiency by switching between them according to link conditions, [21] and [38] use a low power radio to wake up high power ones, [43] and [49] exploit duty-cycling to shut down a wireless radio between transmissions, [37] and [52] compress data before transmission for reducing the power consumed by wireless radios, [31] and [45] tune the transmitted RF power when SNR is sufficient for data communication, and so on. Braidio is radically different in that it enables true asymmetric operation by providing carrier-of-foad capability.

Our work is also inspired by a number of recent advances in Backscatter communication such as the use of ambient RF signals for backscatter [36], low-power high-speed backscatter by optimizing the underlying communication protocol [29, 30, 50, 54], the use of existing wireless radios and infrastructure for backscatter [28, 34], improved coding technique and hardware design [41], design of low power R-FID readers [39] as well as high order modulation schemes such as 16QAM [48]. We also build on the experiences and ideas that have come out of the extensive recent research new hardware platforms for backscatter and self-interference cancellation including full duplex wireless [24, 25, 32], and backscatter tag designs such as Moo [53] and WISP [46, 47].

8. CONCLUSION

To conclude, we present Braidio, a radically new design for a radio that can operate across active and passive modes, and addresses the increasing asymmetry in energy availabil-

ity as devices become smaller. This is a first-of-its-kind device, and one that we believe can be a powerful new addition to the suite of power management techniques that we use on mobile devices. The core innovation is our ability to perform carrier offload, thereby shifting the cost of communication to either end point. By multiplexing between different offloading modes, Braidio can support transmitter to receiver power ratios between 1:2546 to 3546:1, spanning seven orders of magnitude. We show that Braidio increases the number of bits exchanged between a transmitter and receiver by more than two orders of magnitude over Bluetooth, particularly in highly asymmetric scenarios.

Acknowledgement

We thank our shepherd Suman Banerjee and the anonymous reviewers for their insightful comments. This research was partially funded by NSF grants CNS-1218586, CNS-1217606 and NIH 1R01MH109319-01.

9. REFERENCES

- [1] Ams as3992 reader ic. <http://ams.com/eng/Products/UHF-RFID/UHF-RFID-Reader-ICs/AS3992>.
- [2] Ams as3993 reader ic. <http://ams.com/eng/Products/UHF-RFID/UHF-RFID-Reader-ICs/AS3993>.
- [3] Apple iphone 6s hardware specifications. <http://www.apple.com/iphone-6s/specs/>.
- [4] Apple iphone 6s plus hardware specifications. <http://www.apple.com/iphone-6s/specs/>.
- [5] Apple macbook pro 13 inch hardware specifications. <http://www.apple.com/macbook-pro/specs-retina/>.
- [6] Apple macbook pro 15 inch hardware specifications. <http://www.apple.com/macbook-pro/specs-retina/>.
- [7] Apple watch. <https://www.ifixit.com/Teardown/Apple+Watch+Teardown/40655>.
- [8] Cc2541 bluetooth low energy chip. <http://www.ti.com/lit/ds/symlink/cc2541.pdf>.
- [9] Cc2640 bluetooth low energy chip. <http://www.ti.com/lit/ds/symlink/cc2640.pdf>.
- [10] Google nexus 6p technology specifications. https://store.google.com/product/nexus_6p.
- [11] Impinj indy r1000 rfid reader chip. <http://www.impinj.com/products/reader-chips/indy-r1000-rfid-reader-chip/>.
- [12] Impinj indy r2000 rfid reader chip. <http://www.impinj.com/products/reader-chips/indy-r2000-rfid-reader-chip/>.
- [13] Microsoft surface book technology specifications. <https://www.microsoft.com/surface/en-us/devices/surface-book#techspec-block>.
- [14] Ncs2200 low voltage comparator on semiconductor. http://www.onsemi.com/pub_link/Collateral/NCS2200-D.PDF.
- [15] Nike fuel band user manual. <https://support-en-us.nikeplus.com/ci/fattach/get/853467/1406073309/redirect/1d>.
- [16] Pebble watch. <https://www.ifixit.com/Teardown/Pebble+Teardown/13319>.
- [17] Pivothead original. <http://www.pivothead.com/technology/originals/>.
- [18] Thingmagic m6e datasheet. <http://rfid.thingmagic.com/thingmagic-m6e-uhf-rfid-module>.
- [19] Thingmagic m6e micro datasheet. <http://rfid.thingmagic.com/m6e-micro-datasheet>.
- [20] Ts881 nanopower comparator from stmicroelectronics. <http://www.st.com/web/en/resource/technical/document/datasheet/DM00057901.pdf>.
- [21] Y. Agarwal, C. Schurgers, and R. Gupta. Dynamic power management using on demand paging for networked embedded systems. In *ASPDAC'05*, pages 755–759. ACM, 2005.
- [22] S. M. Alamouti. A simple transmit diversity technique for wireless communications. *Selected Areas in Comm., IEEE Journal on*, 16(8):1451–1458, 1998.
- [23] P. Bahl, A. Adya, J. Padhye, and A. Walman. Reconsidering wireless systems with multiple radios. *ACM SIGCOMM CCR*, 34(5):39–46, 2004.
- [24] D. Bharadia, K. R. Joshi, M. Kotaru, and S. Katti. Backfi: High throughput wifi backscatter. In *Proceedings of the 2015 ACM SIGCOMM*, pages 283–296. ACM, 2015.
- [25] D. Bharadia and S. Katti. Full duplex mimo radios. In *NSDI 14*, pages 359–372, 2014.
- [26] D. Bharadia, E. McMillin, and S. Katti. Full duplex radios. In *SIGCOMM CCR*, pages 375–386. ACM, 2013.
- [27] D. C. Cox. Antenna diversity performance in mitigating the effects of portable radiotelephone orientation and multipath propagation. *Communications, IEEE Transactions on*, 31(5):620–628, 1983.
- [28] J. F. Ensworth and M. S. Reynolds. Every smart phone is a backscatter reader: Modulated backscatter compatibility with bluetooth 4.0 low energy (ble) devices. In *RFID'15*, pages 78–85. IEEE, 2015.
- [29] P. Hu, P. Zhang, and D. Ganesan. Leveraging interleaved signal edges for concurrent backscatter. In *Proceedings of the 1st ACM workshop on Hot topics in wireless*, pages 13–18. ACM, 2014.
- [30] P. Hu, P. Zhang, and D. Ganesan. Laissez-faire: Fully asymmetric backscatter communication. In *Proceedings of the ACM SIGCOMM 2015*. ACM, 2015.
- [31] M. Huang, P. E. Caines, and R. P. Malhamé. Uplink power adjustment in wireless communication systems: a stochastic control analysis. *Automatic Control, IEEE Transactions on*, 49(10):1693–1708, 2004.
- [32] M. Jain, J. I. Choi, T. Kim, D. Bharadia, S. Seth, K. Srinivasan, P. Levis, S. Katti, and P. Sinha. Practical, real-time, full duplex wireless. In *MobiCom'11*, pages 301–312. ACM, 2011.
- [33] U. Karthaus and M. Fischer. Fully integrated passive uhf rfid transponder ic with 16.7- μ w minimum rf input

- power. *Solid-State Circuits, IEEE Journal of*, 38(10):1602–1608, 2003.
- [34] B. Kellogg, A. Parks, S. Gollakota, J. R. Smith, and D. Wetherall. Wi-fi backscatter: internet connectivity for rf-powered devices. In *SIGCOMM'14*, pages 607–618. ACM, 2014.
- [35] P. Kyasanur and N. H. Vaidya. Routing and interface assignment in multi-channel multi-interface wireless networks. In *Wireless Communications and Networking Conference, 2005 IEEE*, volume 4, pages 2051–2056. IEEE, 2005.
- [36] V. Liu, A. Parks, V. Talla, S. Gollakota, D. Wetherall, and J. R. Smith. Ambient backscatter: wireless communication out of thin air. In *SIGCOMM CCR*, volume 43, pages 39–50. ACM, 2013.
- [37] F. Marcelloni and M. Vecchio. A simple algorithm for data compression in wireless sensor networks. *Communications Letters, IEEE*, 12(6):411–413, 2008.
- [38] M. J. Miller and N. H. Vaidya. A mac protocol to reduce sensor network energy consumption using a wakeup radio. *Mobile Computing, IEEE Transactions on*, 4(3):228–242, 2005.
- [39] P. V. Nikitin, S. Ramamurthy, and R. Martinez. Simple low cost uhf rfid reader. In *Proc. IEEE Int. Conf. RFID*, pages 126–127, 2013.
- [40] P. V. Nikitin and K. Rao. Antennas and propagation in uhf rfid systems. *challenge*, 22:23, 2008.
- [41] A. N. Parks, A. Liu, S. Gollakota, and J. R. Smith. Turbocharging ambient backscatter communication. In *SIGCOMM'14*, pages 619–630. ACM, 2014.
- [42] T. Pering, Y. Agarwal, R. Gupta, and R. Want. Coolspots: reducing the power consumption of wireless mobile devices with multiple radio interfaces. In *MobiSys'06*, pages 220–232. ACM, 2006.
- [43] J. Polastre, J. Hill, and D. Culler. Versatile low power media access for wireless sensor networks. In *EWSN'04*, pages 95–107. ACM, 2004.
- [44] D. M. Pozar. *Microwave engineering*. John Wiley & Sons, 2009.
- [45] R. Ramanathan and R. Rosales-Hain. Topology control of multihop wireless networks using transmit power adjustment. In *INFOCOM 2000*, volume 2, pages 404–413. IEEE, 2000.
- [46] A. P. Sample, D. J. Yeager, P. S. Powlledge, A. V. Mamishev, and J. R. Smith. Design of an rfid-based battery-free programmable sensing platform. *Instrumentation and Measurement, IEEE Transactions on*, 57(11):2608–2615, 2008.
- [47] J. R. Smith. *Wirelessly Powered Sensor Networks and Computational RFID*. Springer Science & Business Media, 2013.
- [48] S. J. Thomas and M. S. Reynolds. A 96 mbit/sec, 15.5 pj/bit 16-qam modulator for uhf backscatter communication. In *RFID'12*, pages 185–190. IEEE, 2012.
- [49] C. M. Vigorito, D. Ganesan, and A. G. Barto. Adaptive control of duty cycling in energy-harvesting wireless sensor networks. In *SECON'07*, pages 21–30. IEEE, 2007.
- [50] J. Wang, H. Hassanieh, D. Katabi, and P. Indyk. Efficient and reliable low-power backscatter networks. In *Proceedings of the ACM SIGCOMM 2012*, pages 61–72. ACM, 2012.
- [51] C. P. Wen. Coplanar waveguide: A surface strip transmission line suitable for nonreciprocal gyromagnetic device applications. *Microwave Theory and Techniques, Trans. on*, 17(12):1087–1090, 1969.
- [52] L. Xiang, J. Luo, and A. Vasilakos. Compressed data aggregation for energy efficient wireless sensor networks. In *SECON 2011*, pages 46–54. IEEE, 2011.
- [53] H. Zhang, J. Gummesson, B. Ransford, and K. Fu. Moo: A batteryless computational rfid and sensing platform. *University of Massachusetts Computer Science Technical Report UM-CS-2011-020*, 2011.
- [54] P. Zhang, P. Hu, V. Pasikanti, and D. Ganesan. Ekhnnet: high speed ultra low-power backscatter for next generation sensors. In *Proceedings of MobiCom'14*, pages 557–568. ACM, 2014.